J. Astron. Space Sci. 12(1), 1–13 (1995)

SPECTROSCOPIC STUDIES OF STARBURST GALAXIES; THE DYNAMICAL STRUCTURE OF BLUE COMPACT DWARF GALAXY HARO 6 [1]

Mun-Suk Chun
Yonsei University Observatory
Seoul 120-749, Korea

Hong-Kyu Moon and Eon-Chang Sung
Korea Astronomy Observatory
36-1 Whaam-dong, Yuseong, Taejeon 305-348, Korea
email: mschun@galaxy.yonsei.ac.kr, fullmoon@hanul.issa.re.kr, ecsung@hanul.issa.re.kr

(Received April 30, 1995; Accepted May 25, 1995)

ABSTRACT

We carried out photometric and spectroscopic observations of the blue compact dwarf galaxy Haro 6 in the Virgo Cluster of Galaxies. The long-slit spectroscopy was employed at three position angles, $\phi = 0°$, $\phi = 30°$, and $\phi = 120°$ with CCD camera mounted on the Cassegrain Spectrograph. Based on the mean intrinsic axial ratio $< q_o >$=0.3, we derived inclination i of the system as 44° using our composite V-band CCD image. Careful analysis on the velocity field of the system shows an asymptotically flat rotation curve with the maximum rotational velocity $V(r)_{max}$ reaches about 12 km/sec. The calculation of the dynamical mass of Haro 6 with a simple mass model is briefly discussed with emphasis on the mass to luminosity ratio. From the *IRAS Point Source Catalogue*, we derived dust-to-gas ratio which indicates relatively low dust content, thus tempting us to conjecture the youth of the system.

1. INTRODUCTION

Blue compact dwarf galaxies (BCGs) are extragalactic objects with $M_B \geq -18$ which are relatively unevolved systems undergoing intense bursts of star formation at present epoch. Starburst may be defined as a star forming event in a galaxy during which the star formation rate is extreamly higher than normal. The average converting rate of gas into young stars in BCGs is between $\sim$ 0.1 and 1 $M_\odot$ per year. The intense bursts of star formation will give rises to giant extragalactic HII regions and HII galaxies, and the violent

[1]Support for this work was provided by KOSEF and partially by Korea Astronomy Observatory

star formation regions are defined as regions not larger than a few hundred parsecs where tens to thousands of very massive stars($M > 20M_{\odot}$) are formed over time scales of a few tenth of million years.

BCGs have very blue colors in UBV and their optical spectra are dominated by strong narrow nebular emission lines similar to HII regions and indicate the presence of many young ionized OB stars. The lists of emission line galaxies were published by many observers (Maza *et al.* 1991, Arp 1966, Mazzarella and Balzano 1986).

Photometric observations of Haro 6 were made by Thuan and Martin (1981), Sandage and Binggeli (1984), and Gallagher and Hunter (1983). Maza *et al.* (1991) and Gallagher and Hunter (1986) made the low dispersion spectroscopic observations. Thuan and Martin (1981) estimated total magnitude of Haro 6, m_b as 15.25 and colors $B-V$ and $U-B$ as 0.34 and -0.50, respectively. Using the galactic extinction -0.2 and the distance modulus by Jacoby *et al.* (1992), the absolute magnitude M_B of Haro 6 was assumed as -17.3. Haro 6($\alpha_{1950.0} = 12^h12^m.77, \delta_{1950.0} = +6°2'.4, l^{II} = 279°.41, b^{II} = 66°.97$) belongs to the W cloud in the Virgo Cluster. This galaxy was known as various names(CGCG 1212.7+0602, CGCG 041-077, MCG +01-31-030, VCC 144, [RC1] A1213, [RC2] A1212+06, Haro56, IRAS F12127+0602, [MRP91] 121244.8+060221, CTS 1027 and CTS L02.02) and Thuan and Martin (1981) estimated a distance as 25Mpc using the Hubble constant H_o as 75km/sec Mpc^{-1}. In this paper, we emphasize the result of the high dispersion spectroscopy because it was done for the first time on Haro 6, and we could derive a better picture of this galaxy compared to the previous work (Thuan and Martin 1981).

2. OBSERVATIONS

High and low dispersion spectra were obtained by the spectroscopic observations with the 74 inch telescope at the Mount Stromlo Observatory to get the radial velocities and abundances of the blue compact dwarf galaxy Haro 6. Images and surface brightness profiles in various filters were made through the CCD photometric observations using the 1 m telescope at the Siding Spring Observatory.

2.1 High Dispersion Spectra

A Cassegrain spectrograph and a CCD camera attached to the 74 inch telescope at Mount Stromlo Observatory, Australia, were used to get the Hα high dispersion spectra of the Haro 6. Observations were made at the various slit position angles ($\phi = 0°, 30°, 120°$) including the optical major and minor axes. The image scale of the CCD was $0''.72$/pixel. Two standard stars (LTT 4816 and LTT 6284) were also observed and the Fe-Ne comparison arc spectrum was obtained before and after the standard star's spectrum observation. During the observing runs, the seeing was about $2''$. Table 1 lists the characteristics of the telescope and the adopted spectral parameters.

Table 1. The characteristics of the telescope and the adopted spectral parameters.

Parameter		Parameter	
Diameter	1.88m	Slit size	long slit
f ratio	f/18	Central wavelength	6563 Å
Image scale	$0''.72$/pixel	Dispersion	0.36 Å/pixel
CCD size	578×386	Grating	1200 grooves/mm
Pixel size	12 μm^2	Exposure time	1000 sec
Detector	UV coated BCCD	Comparison arc	Fe-Ne
Slit width	$2''.1$		

2.2 Low Dispersion Spectra

A blue PCA (Photon Counting Array) which is attached to the MSO 74 inch telescope was used to get the low dispersion spectra. The grating was 300 grooves/mm, and the blue (3500Å to 5500Å) and red (4700Å to 7000Å) region spectra were observed separately. The slit width was adjusted to minimize the FWHM (Full Width at Half Maximum) of the strong comparison emission He-Ar arc line as 10 Å. The slit was positioned to the direction of east to west and the exposure times were 1,000 seconds, 2,000 seconds in blue and red region, respectively. Figure 1 shows the low dispersion spectra of Haro 6 in blue and red regions. [OII] and [OIII] forbidden lines are very strong and [NII] $\lambda\lambda$ 6548, 6563 and [SII] $\lambda\lambda$ 6717, 6731 lines show the doublet features.

2.3 CCD Photometry

To get the dynamical and population structures from the surface brightness distribution of Haro 6, we had $UBVRI$ and Hα CCD images using 1m telescope at the Siding Spring Observatory. Exposure times varied in the range of 300 to 500 seconds for each filters. The image scale was $0''.57$/pixel and the seeing was less than $2''$ during the observing runs. Figure 2 shows the isophotal contour maps of UBV and R filter bands. The envelope of Haro 6 galaxy becomes clear to the longer wavelength filter band. Each figures have the same angular sizes ($57'' \times 57''$).

3. REDUCTIONS

Using the IRAF (Image Reduction and Analysis Facilities) developed by NOAO (National Optical Astronomy Observatories), we made reductions of observed spectra of Haro 6 as the following procedure.

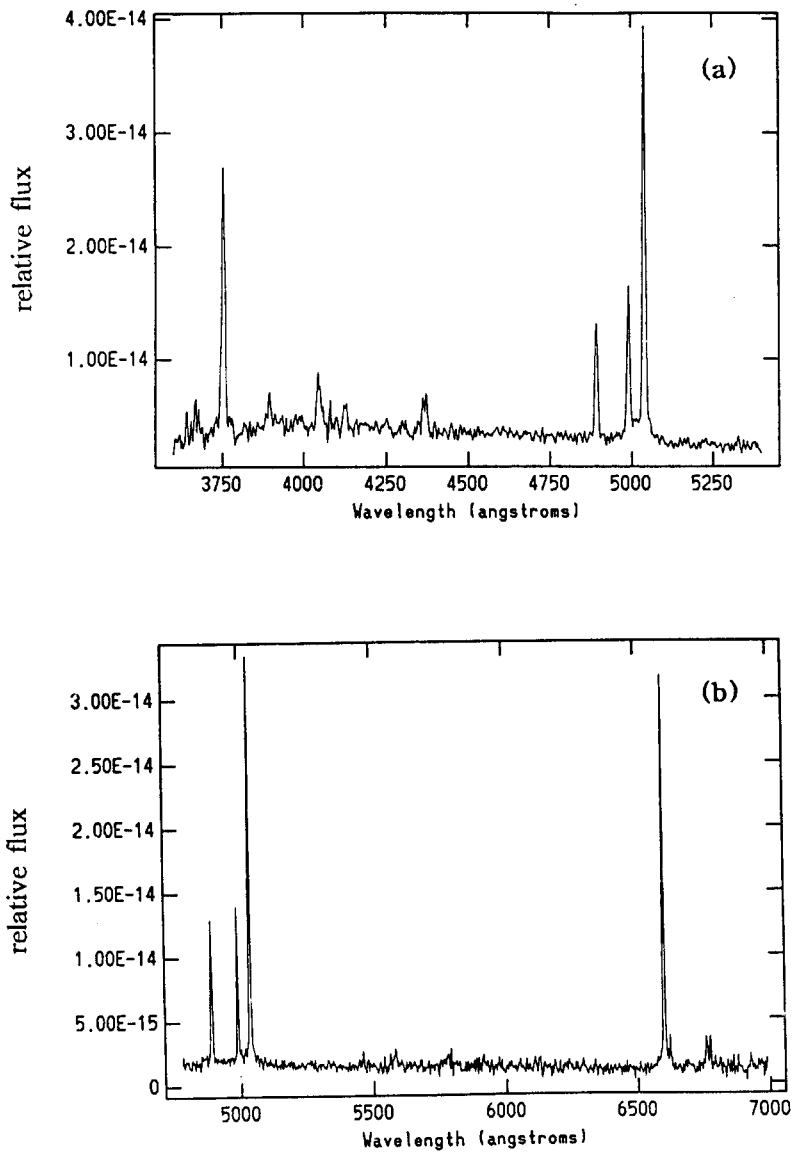

Figure 1. (a) Low dispersion spectra of Haro 6 at blue region, (b) Low dispersion spectra of Haro 6 at red region.

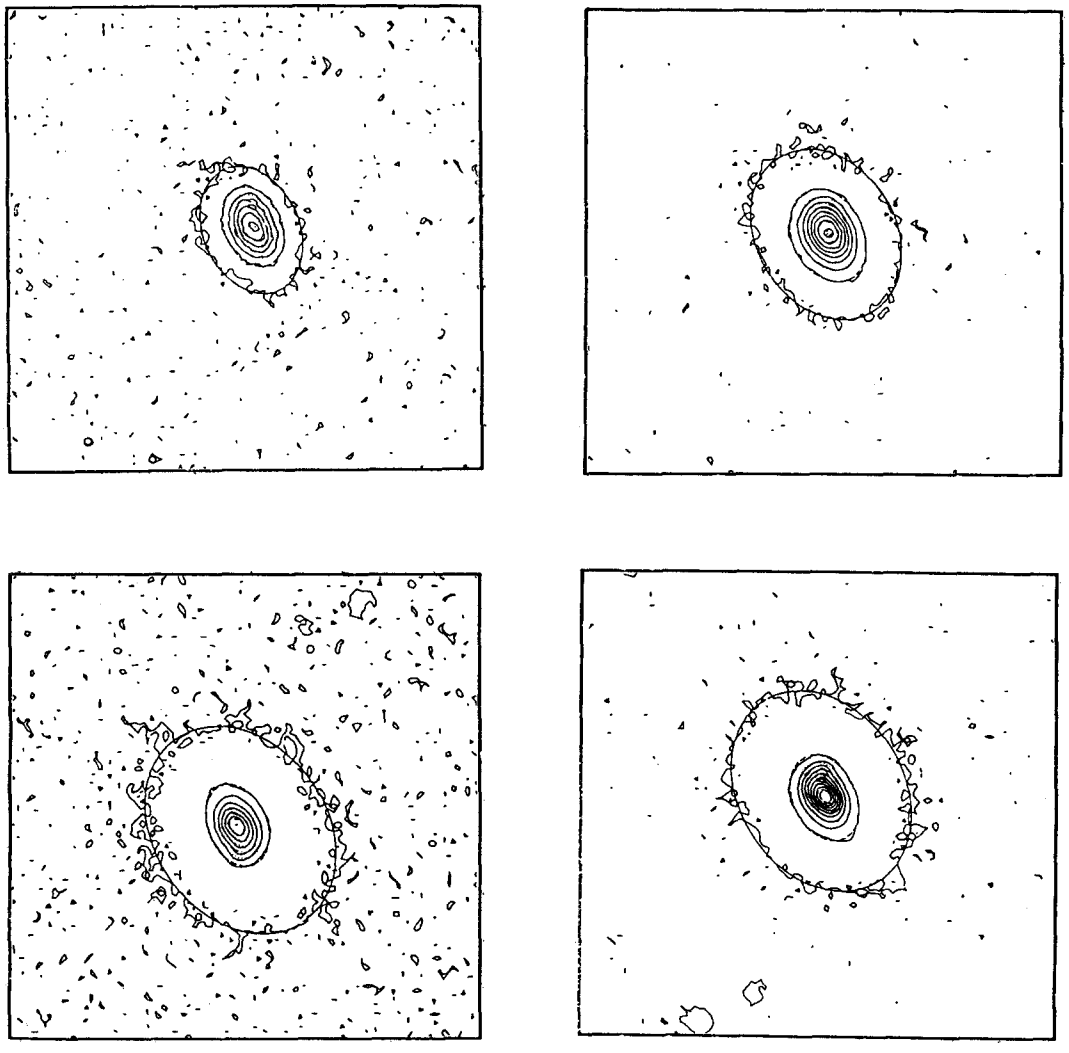

Figure 2. Isophotal contour maps of Haro 6 in U (upper left), B (upper right), V (lower left), and R (lower right) band images.

1. Bias subtraction: Bias subtraction was made after the bias level was subtracted from the overscan region of the CCD image.
2. Trimming: We used the CCD image regions where the intensity is above 70% of the maximum intensity.
3. Flat field correction: Sky flat images were obtained from the exposures of the twilight sky. The response functions were obtained from the combined flat field images to carry out the flat field correction to the observed images.
4. Slit profile and illumination correction: Even the small scale structure was removed from the flat field correction, there still remains the large scale structure on the slit axis and dispersion axis due to the transmission variation at the spectrum. To eliminate these effects we divided observed spectra into 5 to 10 regions to their wavelengths and made the polynomial fitting to the slit axis at each divided wavelength region.
5. Distortion correction: Distortion correction of the observed spectrum was made using the identification of the Ne-Fe arc spectrum. We rectified the correction process after applying the distortion map to each images.
6. Sky subtraction and fluxing: Absolute flux was made through the process of the sky subtraction, extinction correction of the earth atmosphere and the brightness correction to the wavelength using the flux standard star.
7. Gaussian fitting: Some emission lines were fitted to the Gaussian function to get radial velocities. When the signal to noise ratio is big enough, we used the centroid finding algorithm. The other cases we used Gaussian curve fitting algorithm to the edge of spectrum. Figure 3 shows examples of the Gaussian fitting to an observed spectrum.

4. DISCUSSION

4.1 Radial Velocity at $\phi = 120°$ and $\phi = 0°$

Figure 4 shows radial velocity, relative flux and FWHM to the radial distance in Haro 6 at $\phi = 120°$. Until R $\leq 5''$ there seems to exist a solid body rotation and afterward it becomes to decline. However, it is uncertain to assume this tendency as a real one because the rate of declination is in the range of fluctuation. However the FWHM to the radial distance does not show any significant variation. Overall tendency of velocities, relative flux and FWHM to the radius at both slit position $\phi = 0°$ and $\phi = 120°$ are similar each other (cf. Figure 5).

4.2 Radial Velocity at $\phi = 30°$

Generally, a rotation feature at the dynamical minor axis in a disk galaxy does not exist. As the optical major axis coincides to the dynamical major axis in Haro 6, velocity value at

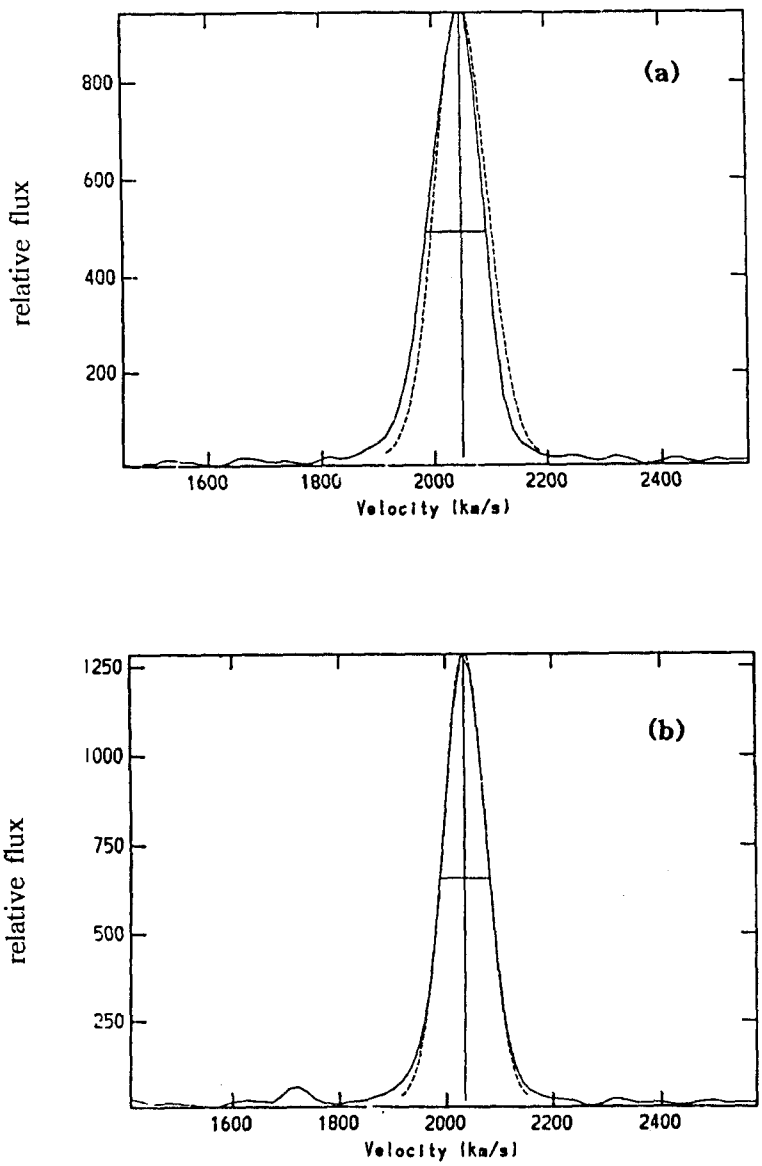

Figure 3. Examples of the Gaussian function fitting to an observed spectrum.

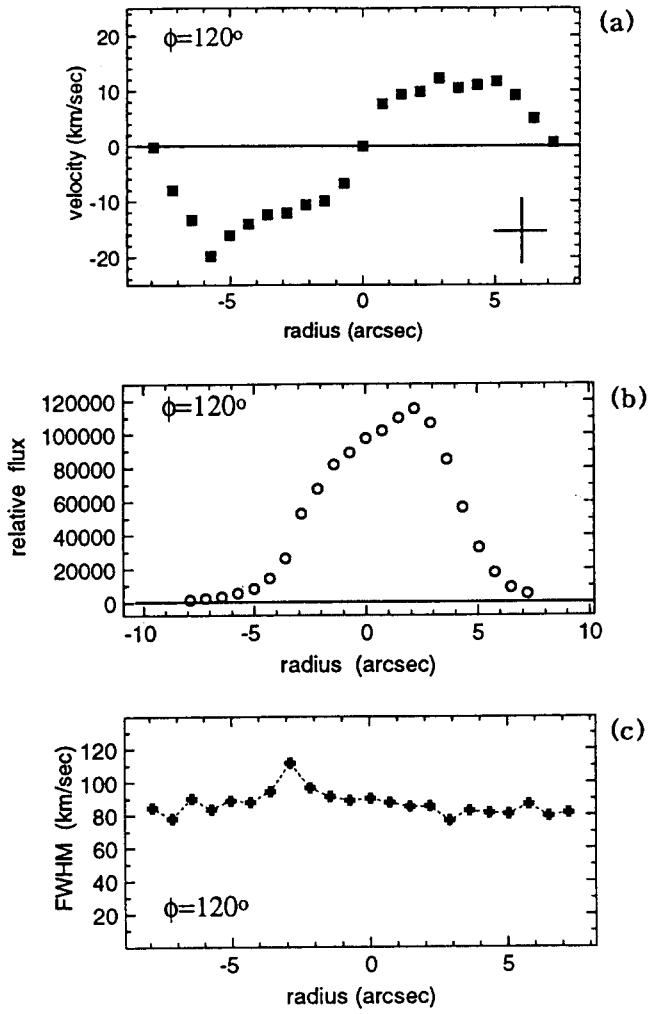

Figure 4. Radial velocity, relative flux and FWHM to the radial distance in Haro 6 at $\phi = 120°$.

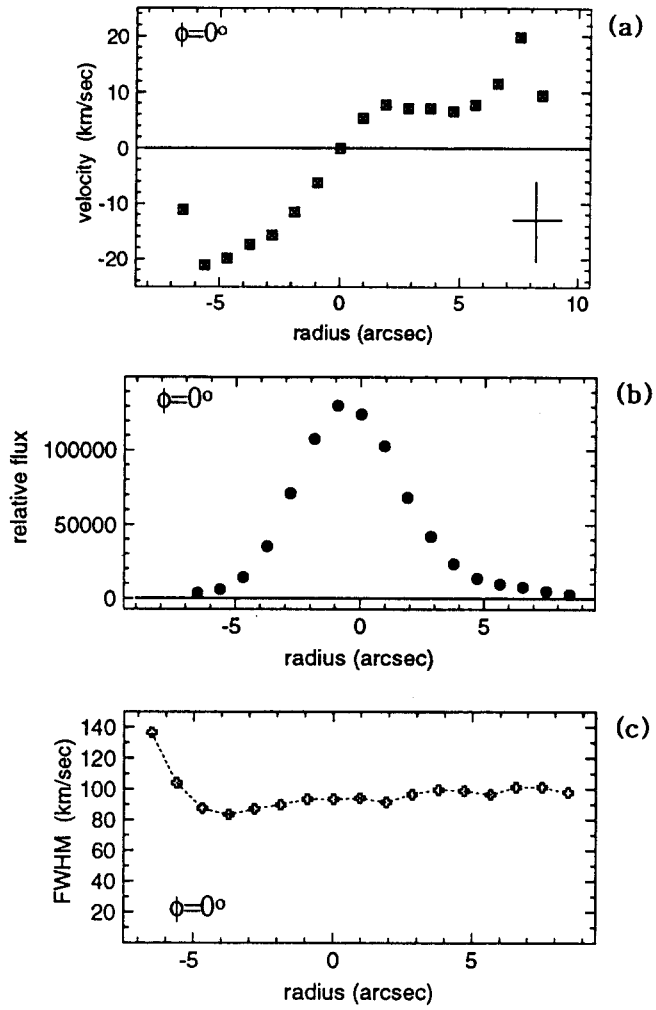

Figure 5. Radial velocity, relative flux and FWHM to the radial distance in Haro 6 at $\phi = 0°$.

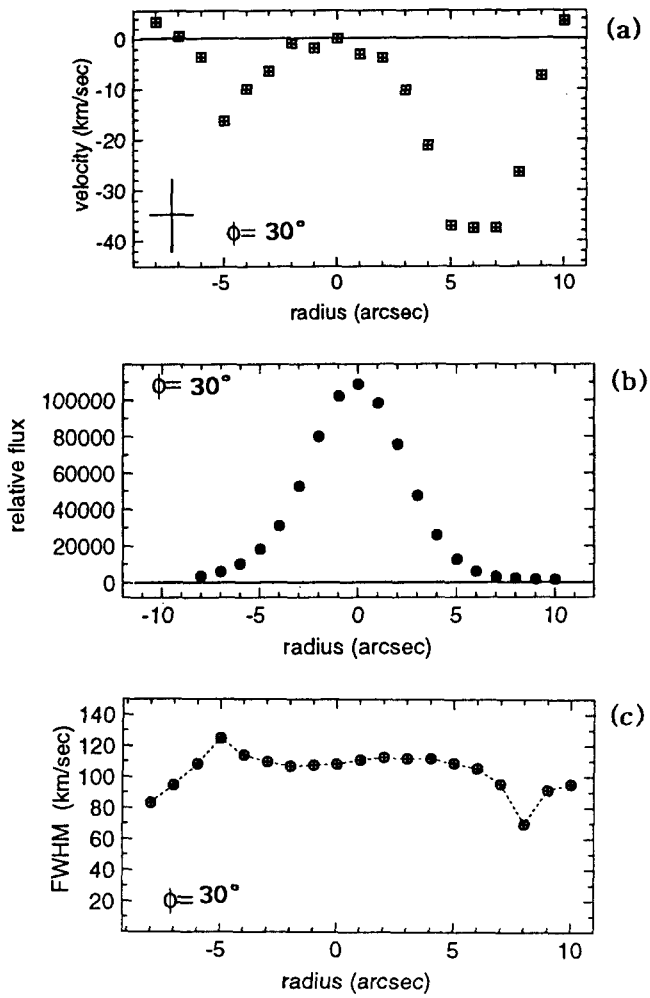

Figure 6. Radial velocity, relative flux and FWHM to the radial distance in Haro 6 at $\phi = 30°$.

$\phi = 30°$ should be 0. However, as in Figure 6, radial velocities at R $\sim \pm 5''$ are observed as -20 km/sec and -40 km/sec each other. The average value of FWHM is about 110 km/sec which is larger (about 30 km/sec) than that at $\phi = 0°$ and $\phi = 120°$. From this observed velocity, we assume that there exists larger random motion at the minor axis than the other position.

4.3 Inclination of the Disk

The isophotal maps in Hα and $UBVRI$ show well defined elliptical structure of Haro 6 (cf. Figure 2). Using the composite V-band CCD image of Haro 6, we determined the apparent axial ratio, q , of the ellipse with the isophotal magnitude of 25 mag/arcsec^2 as 0.75. With the mean intrinsic axial ratio $< q_o >$=0.3 for the dwarf galaxies (Gordon 1979), we derived the inclination of the Haro 6 as 44° using the methods of Thuan and Martin (1981).

4.4 Rotation Velocity Curve and Mass Estimation

Radial velocities at $\phi = 120°$ were fitted to the rotation velocity curve model of Bertola *et al.* (1981) with the maximum velocity V_{max}(R) $\sim$ 12 km/sec as in Figure 7. The model fitting was in good agreement with the observed ones. Mass distribution M(R) and density distribution ρ(R) were estimated from the rotation curve of Haro 6 using the methods of Bertola *et al.* (1991). Assuming the flat rotation to the other regions, the mass of Haro 6 until the optical radius R $\sim 17''$ was calculated as $\sim 7 \times 10^8 M_\odot$. As the luminosity is $\sim 4.2 \times 10^8 L_\odot$, the mass to light ratio M/L$_B$ is 1.7 which is the typical value of BCGs.

4.5 Total Dust Mass and Dust-to-Gas Ratio

IRAS Point Source Catalogue was used to derive the infrared luminosity and dust mass in Haro 6. The infrared luminosity L_{FIR} was calculated as $\sim 1.64 \times 10^8 L_\odot$ using the flux data at 60μm and 100μm, and the luminosity ratio L_{FIR}/L_B as $\sim$ 0.4. The far infrared luminosities of Haro 6 shows the black body radiation of temperature $T_{BB} \sim 75K$. Then we calculated the total dust mass of Haro 6 as $M_d \sim 6 \times 10^2 M_\odot$ and the dust-to-gas ratio as $\sim 10^{-6}$ by using the methods of Telesco and Harper (1980). This seems to be related with the age of the galaxy. Because the stars are not evolved enough to eject dusts to the galaxy, we observe the lack of the far infrared radiation of the Haro 6 (Gondhaleker *et al.* 1986). According to the photometric evolution model of galaxies by Struck-Marcell and Tinsley (1978), star burst age of galaxies can be derived from the $U - B$ color index. We calculated the star burst age of Haro 6 as only $\leq 5 \times 10^7$ years from the $U - B = -0.46$.

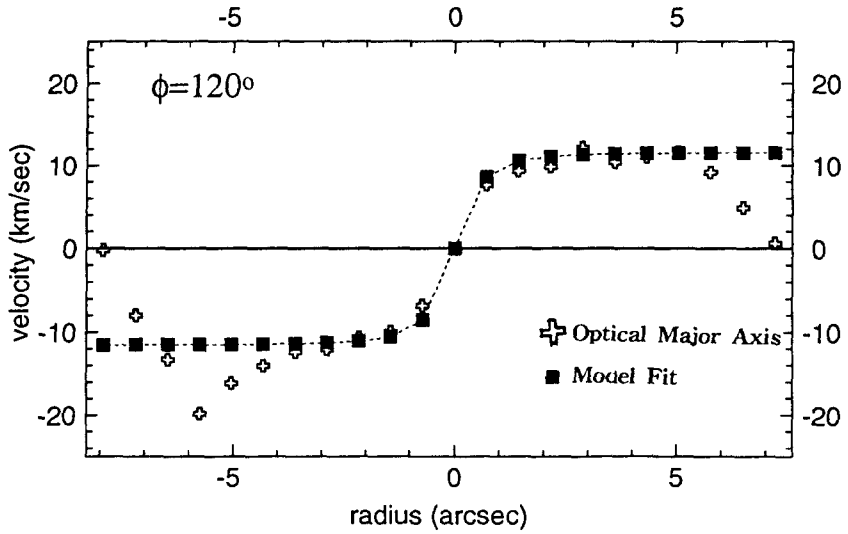

Figure 7. Model fitting of the rotation velocity curve to the theoretical one with the maximum velocity $V_{max} \sim$ 12km/sec.

5. CONCLUSION

We studied the dynamical structure of blue compact dwarf galaxy Haro 6 using the photometric CCD images, high and low resolution spectra and *IRAS Point Source Catalogue*. We determined the apparent axial ratio q_{25} as 0.75 and the inclination as 44°. The low dispersion spectra show the typical feature of blue compact dwarf galaxies. In the central part of this galaxy, we detected very strong Hα flux which comes from the giant HII region in the galaxy. The long-slit high dispersion spectroscopy was employed at three position angles of the galaxy, $\phi = 0°$, $\phi = 30°$, and $\phi = 120°$. On the dynamical semi-major axis($\phi = 120°$), a flat rotation is appeared with the maximum velocity $V_{max} \sim$ 12km/sec. The rotation feature to the axis at $\phi = 0°$ is very similar with the major axis. However, turbulence motion dominates on the direction of minor axis at $\phi = 30°$. The virial mass of Haro 6 was caculated from the radial velocity curve fitting to the dynamical model as $\sim 7\times10^8 M_\odot$ within the optical radius $\sim 17''$. In this region, the mass to light ratio(M/L_B) is 1.7 in solar unit. Infrared luminosity and dust mass of Haro 6 were derived from *IRAS Point Source Catalogue* data as $L_{FIR} \sim 1.64 \times 10^8 L_\odot$ and $M_d \sim 6.48 \times 10^2 M_\odot$, respectively. Then we derived luminosity ratio L_{FIR}/L_B as $\sim$ 0.4 and the dust-to-gas mass ratio as $\sim 10^{-6}$. The lack of infrared radiation in Haro 6 indicates that this galaxy is very young

system with the star bust age of only $\leq 5 \times 10^7$ years, which is derived from the photometric evolution models.

ACKNOWLEDGEMENTS: Support for this work was provided by KOSEF (grant number 941-0400-001-2). ECS acknowledges partial support by Basic Research Fund of Korea Astronomy Observatory. We are indebted to Professor K. C. Freeman for his advice and help. We appreciate assistance of staffs at Mount Stromlo and Siding Spring Observatories.

REFERENCES

Arp, H. C. 1966, Atlas of Peculiar Galaxies (California Institude of Technology, Pasadena)
Bertola, F., Bettoni, D., Daniger, J., Sadler, E., Sparke, L. & De Zeeuw, T. 1991, ApJ, 373, 369
Gallagher, J. S. & Hunter, D. A. 1983, ApJ, 274, 41
Gallagher, J. S. & Hunter, D. A. 1989, AJ, 98, 806
Gondhaleker, P. M., Morgan, D. H., Dopita, M. & Ellias, R. J. 1986, MNRAS, 219, 505
Gordon, D. 1979, Ph.D Thesis, University of Florida
Jacoby, G. H., Branch, D., Ciardllo, R., Davies, R. L., Harris, W. E., Pierce, M. J., Pritchet, C. J., Tonry, J. L. & Welch, D. 1992, NOAO Preprint No.433
Maza, J., Ruiz, M. T., Pena, M., Gonzalez, L. E. & Wischnjewsky, M. 1991, A&AS, 89, 389
Mazzarella, J. & Balzano, V. 1986, ApJS, 62, 751
Sandage, A. & Bingglei, B. 1984, AJ, 89, 919
Struck-Marcell, C. & Tinsley, B. M. 1978, ApJ, 221, 562
Telesco, C. M. & Harper, D. A. 1980, ESO preprint No.95
Thuan, T. X. & Martin, G. E. 1981, ApJ, 247, 823